Supplementary Material

Methods

Microarrays & Ingenuity Pathway Analysis

RNA concentration was measured using a Nanodrop ND-1000 and RNA integrity was assessed using the Bioanalyzer 2100 (Agilent). Total RNA was labeled on a sample-by-sample basis according to manufacturer's guidelines for use with the Affymetrix Human Gene 1.0 ST Array (Affymetrix, Inc). Labeled cRNA were hybridized to these arrays in blinded interleaved fashion. The Affymetrix scanner 3000 was used in conjunction with Affymetrix GeneChip Operation Software to generate one .CEL file per hybridized cRNA. These files have been deposited in NCBI GEO (http://www.ncbi.nlm.nih.gov/geo/) and are available for download (GSE66988). The Affymetrix Expression Console was next used to summarize the data contained across all .CEL files and generate 33,297 RMA normalized gene fragment expression values per file. Quality of the resulting values was challenged and assured via Tukey box plot, covariance-based PCA scatter plot, and correlation-based heat map using functions supported in "R" (www.cran.r-project.org). Lowess modeling of the data (CV~mean expression) was performed to characterize noise for the system and discard gene fragments having noise-biased data (all RMA expression values < 7). For gene fragments not discarded, differential expression across sample classes was tested for via ANOVA under BH FDR MCC condition (alpha = 0.05). Gene fragments having a corrected $p<0.05$ by this test were subset and post hoc analysis performed using the TukeyHSD test. Gene fragments with a $p<0.05$ by this test and an absolute difference of means ≥ 1.5 for a class comparison were subset as those having differential expression between those classes respectively. Gene annotations for these subset fragments were obtained from Ingenuity Pathway Analysis (www.ingenuity.com) as were the corresponding enriched functions and pathways. Ingenuity Pathway Analysis software was used to create diagrams for comparing biological pathways and determining canonical pathways. "Core Analysis" was performed on the gene fragments having a corrected $p<0.05$ in both young HVs and MS patient monocytes to determine the canonical pathways significantly affected by myelin debris phagocytosis and disease status using a right-tailed Fisher Exact Test. The software determines these significant pathways based on the 1) known list of genes in that pathway, 2) the total number of genes in our platform, and 3) the number of significantly altered genes in both our dataset and a given pathway. $p<0.05$ for the genes

differentially regulated in the given pathway. The threshold (>1%) represents that these pathways have a $p<0.01$. Additionally, the Ratio indicates the ratio of genes enriched in our pathway compared to the total number of known genes in that pathway.

PCR Arrays and qPCR

Isolated RNA was converted to cDNA using the QuantiTect Reverse Transcription Kit (Qiagen). cDNA from 8 samples/group (for conventional PPARγ qPCR) and pooled from 6 samples in each group (for PCR Arrays) was added to SYBR Green qPCR SuperMix (Bio-Rad). For Human PPAR Targets PCR Array (SABiosciences), pooled samples were added to plates with primer pairs for 84 genes in the PPAR pathway. For qPCR analysis of PPARγ, Forward primers: AGT CCT CAC AGC TGT TTG CCA AGC and Reverse primers: GAG CGG GTG AAG ACT CAT GTC TGT C (IDT DNA) were added to cDNA/SYBR Green mixes. Plates were run on a CFX96 Detection System (Bio-Rad). Data normalization was performed using Excel 2010. Relative quantification was used to compare samples to untreated controls, resulting in ΔCt values used to calculate relative fold changes. The genes significantly affected by MS disease state and pioglitazone treatment ($|FC| > 1.5$) were plotted.

Electrochemiluminescence immunoassays (ECLIA)

The standard protocol for the developed assays was as follows using the MesoScale Discovery system; standard binding plates were coated with 30 µl of working solution of capture antibody (R&D Systems, MAB3833) and stored at 4 °C overnight. The next morning, the coating solution was aspirated, and plates were blocked with 150 µl of 1% BSA in PBS 1X for 2h at RT on a shaker at 200 rpm. After washing plates 3 times with PBS-T, 25 µl of each supernatant sample was added to each well, and the plates were incubated for 2h at RT on a shaker at 200 rpm. Plates were washed again 3x with PBS-T. 25 µl of working solution of detection antibody (R&D Systems, BAF383) was added to each well, and the plates were incubated as above. The plates were then washed and incubated 1h with 25 µl of 0.25 µg/ml Sulfo-tag labeled Streptavidin solution (MesoScale Diagnostics). Finally, plates were washed 3 times with PBS-T and 150 µl of 2 fold-concentrated Read Buffer was added for the SI2400 image analyzer (MesoScale Diagnostics). The standard curve was generated from a serial dilution of standard proteins in 1% BSA in PBS with CVs <20%.

A)

	Number of Subjects		
	Young HV	Old HV	MS Patients
Overall Population	36	36	70
Baseline demographic factors			
Sex			
Men	20	22	29
Women	16	14	41
Age			
≤40 years	36	0	20
>40 years	0	36	50
Race			
Caucasian	20	28	62
Other	16	8	8
Previously Treated			
No	36	36	32
Yes	0	0	38
Daclizumab			*8*
Idebenone/Placebo			*14*
Rituximab			*8*
Other			*8*

B)

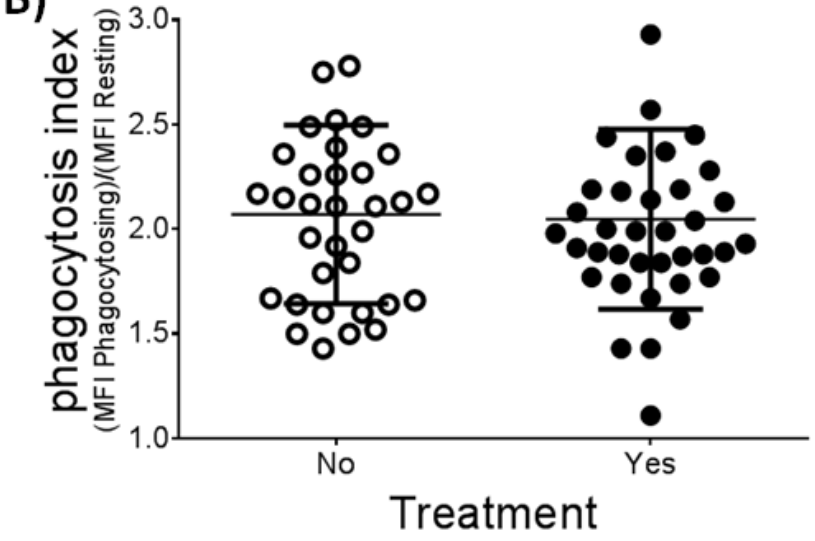

Supplementary Figure 1. Demographic data for healthy volunteers (HV) and MS patients. A) Demographic characteristics, including age, race, gender, and history of treatment with disease modifying therapies, for the three subject groups (young HV, old HV, and MS patients). B) Pre-treatment of patients with disease modifying MS drugs did not significantly affect the phagocytosis index.

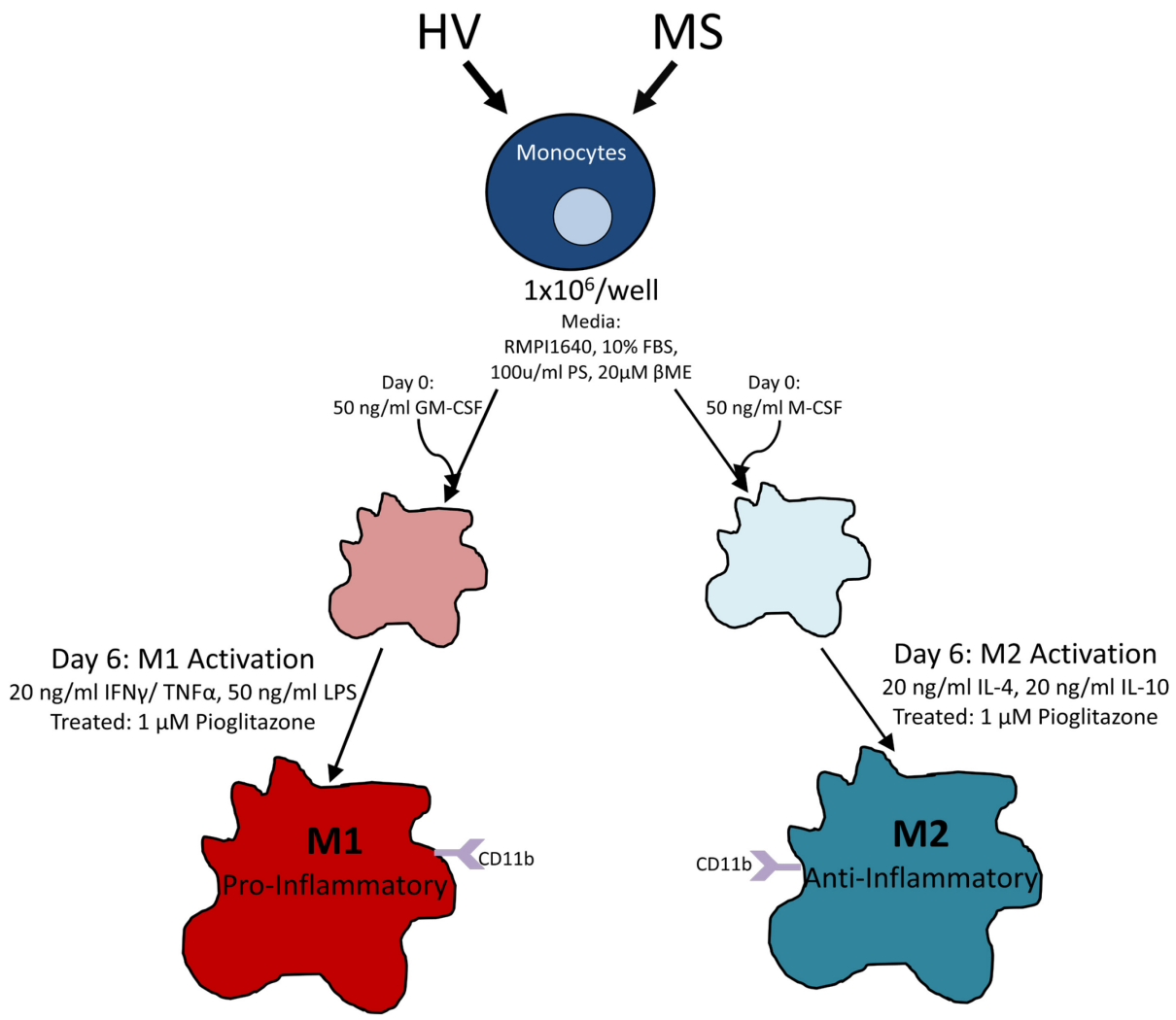

Supplementary Figure 2. M1/M2 macrophage polarization from human CD14+ monocytes. Cells were cultured and differentiated for 7 days in pro- and anti-inflammatory conditions towards M1 and M2 polarization. Effects of pioglitazone treatment and myelin debris phagocytosis on CD163 expression on CD11b+ macrophages were determined by flow cytometry.

Supplementary Table 1. Genes important in monocyte function and phagocytosis are dysregulated in MS patient monocytes. Ingenuity pathway analysis was used to determine genes changed in the top canonical pathways in MS patients.

	Fold Δ in MS Patients vs HVs		**Fold Δ in MS Patients vs HVs**
IL-17 Signalling & MS Pathogenesis			
CCL20	3.37	CXCL3	2.39
CXCL1	2.23	CCL5	2.00
CXCR4	-2.95	SDC4	1.90
Pattern Recognition Receptors, TREM1, & TLR Signalling			
NLRP3	2.27	SOCS3	2.55
RIPK2	1.63	SRF	1.63
TRAF1	1.88	TLR1	-1.98
Immunological Diseases			
TGFBR1	-1.51	GBP1	2.28
STAT4	3.09	TNFSF15	2.44
CXCR4	-2.95	GFTP1	-1.75
ARL5B	1.53	MS4A4A	1.79
CCRN4L	2.17	TBC1D2	-1.83
CLEC4E	1.60		
Lipid Metabolism			
ACAT2	1.72	LIPA	-1.53
BTG2	1.54	LPL	1.97
EDN1	2.23	NR4A1	2.12
GBP2	2.15	PRLR	-1.83
Actin Rearrangement			
CD180	-3.81	GFPT1	-1.75
DUSP16	1.67	NFKBIZ	1.63
E2F7	3.85	NLRP3	2.27
GBP3	2.99	ZC3H12A	1.87

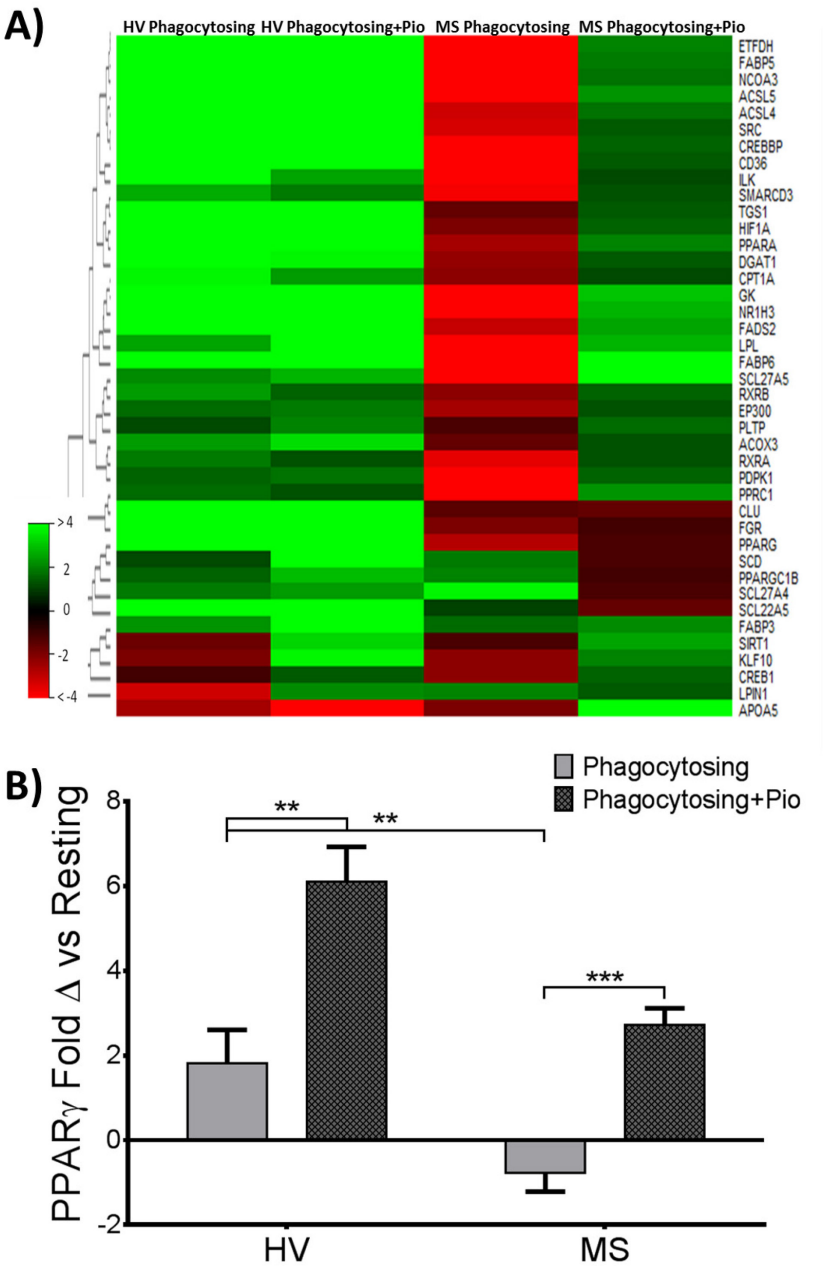

Supplementary Figure 3. Pioglitazone reverses impaired expression and activation of PPARγ pathways in MS patient monocytes. Monocytes from HV and MS patients were treated with myelin debris and pioglitazone, and cDNA was isolated. A) The PPAR Targets PCR Array (SABiosciences) was used to determine changes in genes in the PPAR pathway. Fold changes were calculated by comparing HV or MS cells to resting controls. The heat map depicts genes in the PPAR pathway with |FC| > 1.5, showing PPAR-related genes upregulated in phagocytosing HV monocytes compared to phagocytosing MS patient cells. Pioglitazone enhanced expression of genes in the PPAR pathway in MS monocytes. Green=upregulated, Red=downregulated, n=6/group. B) Fold changes in PPARγ expression were determined by conventional qPCR. PPARγ expression is significantly greater in phagocytosing HV monocytes compared to MS patients, and expression increased after pioglitazone treatment in both HV and MS monocytes. Two-way repeated-measures ANOVA with Tukey's test, **p<0.01, ***p<0.001, n=8/group.

Supplementary Table 2. Proteins in MS patient monocyte supernatants affected by myelin phagocytosis and pioglitazone treatment (relative to resting controls). Using SOMAscan technology, pioglitazone was found to enhance several proteins involved in antioxidant functions, anti-inflammatory activation of monocytes, and growth factor signalling.

Target Full Name	ENTREZ Gene Symbol	Function	Phagocytosing		Pioglitazone	
			Δ	SD	Δ	SD
Bone morphogenetic protein receptor type-1A	BMPR1A	Activin receptor/Activated by TGFB (1)	1938.32%	336.67%	2450.38%	584.93%
Contactin-1	CNTN1	Cell adhesion molecule in IgG superfamily	1352.20%	5.80%	1625.51%	107.15%
Integrin alpha-I: beta-1 complex	ITGA1	Collagen receptor, Monocyte adhesion/differentiation (2)	772.98%	158.21%	952.41%	246.23%
Protein kinase C gamma type	PRKCG	PKC protein, Stimulates neuronal functions	380.83%	96.31%	413.79%	254.97%
Phosphatidylethanolamine-binding protein 1	PEBP1	Inhibits NFkB signaling and promotes M2 (3)	262.93%	7.63%	344.58%	87.06%
Tissue factor pathway inhibitor	TFPI	Released by monocytes, inhibits LPS response (4)	64.49%	13.78%	305.32%	50.85%
Cytochrome c	CYCS	Heme protein transfer to cytochrome oxidase	187.37%	32.09%	260.89%	76.57%
Low affinity immunoglobulin epsilon Fc receptor	FCER2	B cell specific antigen & IgE receptor, promotes growth	68.35%	2.49%	228.77%	55.36%
Antithrombin-III	SERPINC1	Inhibitor of coagulation and NFkB (5)	93.13%	12.05%	227.66%	103.81%
Complement component C9	C9	Part of membrane attack, kills bacterial cells on release	82.16%	8.45%	173.89%	95.46%
Cathepsin A	CTSA	Associates with protease, faster debris breakdown	68.09%	10.03%	170.51%	56.05%
Ferritin, heavy polypeptide 1	FTH1	Fe storage in remyelination (6); antioxidant	81.63%	41.31%	166.16%	42.19%
C-C motif chemokine 7	CCL7	Monocyte chemoattractant protein 3	102.80%	4.37%	143.96%	21.37%
Gro-beta/gamma	CXCL3	Recruits neutrophils, promotes inflammation	39.82%	6.82%	142.10%	47.37%
Coagulation factor IX	F9	Clotting factor, Antioxidant protein (7)	69.66%	37.88%	138.86%	84.56%
Thrombin	F2	Clotting, elicits chemotaxis, Antioxidant	63.41%	8.16%	135.91%	31.11%
Tenascin	TNC	ECM protein, activation in macrophages (8)	44.14%	17.78%	120.14%	38.22%
C-C motif chemokine 2	CCL2	Monocyte chemoattractant protein	62.26%	10.96%	117.33%	18.84%
Nucleoside diphosphate kinase B	NME2	Activator of MYC, M2 differentiation (9)	100.00%	7.86%	115.87%	38.21%
Complement C3b	C3	Released by myelin-phagocytosing monocytes, Resolves inflammation (10, 11)	42.82%	16.41%	108.36%	33.66%
Intercellular adhesion molecule 5	ICAM5	Glycoprotein that binds to leukocyte adhesions proteins	87.72%	49.44%	103.50%	50.45%
C-C motif chemokine 18	CCL18	Upregulated by IL4 release by M2 cells (12)	68.07%	4.87%	100.94%	43.22%

Metalloproteinase inhibitor 1	TIMP1	Inhibitor of pro-inflammatory MMPs, Inversely correlated with MMP 9 in MS (low TIMP1) (13)	19.93%	0.10%	99.31%	22.00%
Inhibin beta A chain	INHBA	Forms homodimer to create Activin A glycoprotein	65.85%	2.29%	96.53%	47.85%
Complement factor B	CFB	Combines with C3 (see above)	45.43%	8.08%	94.03%	55.67%
Carbonic anhydrase 1	CA1	Antioxidant, regulated by RXR signaling (14, 15)	53.84%	15.33%	93.82%	43.85%
Urokinase plasminogen activator surface receptor	PLAUR	Localizes and promotes plasmin formation	35.05%	16.44%	93.52%	1.12%
Peroxiredoxin-1	PRDX1	Antioxidant enzyme, reduces ROS and inflammation	77.22%	1.43%	87.37%	28.33%
Brevican core protein	BCAN	Chondroitin sulfate proteoglycan membrane protein	59.74%	13.54%	73.48%	18.24%
Protein kinase C beta type (splice variant beta-II)	PRKCB	PKC protein, PMA-activated, cytokine stimulation (16)	73.70%	12.53%	69.84%	15.97%
Reticulon-4 receptor	RTN4R	Receptor for Oligodendrocyte myelin glycoprotein	52.82%	14.06%	59.82%	12.21%
Tyrosine-protein phosphatase non-receptor type 11	PTPN11	Dephosphorylates ROCK2, actin polymerization (17)	39.64%	12.79%	55.89%	19.77%
Ephrin type-B receptor 6	EPHB6	Inhibits IL2 secretion (18)	39.68%	2.36%	47.35%	4.27%
Calcineurin	PPP3CA	Increases IL2/NFAT (19)	40.70%	9.70%	45.96%	11.84%
Contactin-2	CNTN2	IgG superfamily, Cell adhesion molecule	51.41%	0.16%	45.06%	12.48%
Histone H1.2	HIST1H1C	Histone chromatin remodeling	32.02%	6.79%	43.72%	28.47%
Protein 4.1	EPB41	Actin rearrangement and cytoskeletal protein	42.10%	6.65%	40.03%	30.75%
Neutrophil-activating peptide 2	PPBP	Growth factor, chemoattractant for neutrophils	0.71%	14.99%	35.36%	21.35%
Transforming growth factor-beta-induced protein ig-h3	TGFBI	Induced by TGFB signaling , modulates cells adhesion	1.37%	1.46%	25.18%	1.57%
C-C motif chemokine 1	CCL1	Chemotactic activity for monocytes	-8.16%	7.68%	-28.87%	10.75%
Legumain	LGMN	Produced on LPS activation in dendritic cells	-13.03%	0.97%	-31.70%	5.87%
Glutathione S-transferase A3	GSTA3	Reducing agent	-20.93%	2.64%	-32.07%	12.34%
Matrix metalloproteinase-9	MMP9	Pro-inflammatory enzyme released in MS lesions and associated with worsening of disease (20)	3.28%	2.91%	-32.63%	17.29%
Urokinase-type plasminogen activator	PLAU	Cleaves plasminogen to degrade clots	19.95%	10.61%	-34.16%	20.52%
SLAM family member 7	SLAMF7	M1 protein, Up in MS (21, 22)	-13.64%	8.77%	-35.19%	14.80%
Neurogenic locus notch homolog protein 3	NOTCH3	Enhances M1 macrophage activation (23)	-7.39%	1.79%	-37.58%	2.54%

References

1. Miron VE, Boyd A, Zhao JW, Yuen TJ, Ruckh JM, Shadrach JL, et al. M2 microglia and macrophages drive oligodendrocyte differentiation during CNS remyelination. Nature neuroscience. 2013.
2. Becker HM, Rullo J, Chen M, Ghazarian M, Bak S, Xiao H, et al. α1β1 integrin-mediated adhesion inhibits macrophage exit from a peripheral inflammatory lesion. The Journal of Immunology. 2013;190(8):4305-14.
3. Granovsky AE, Rosner MR. Raf kinase inhibitory protein: a signal transduction modulator and metastasis suppressor. Cell Res. 2008;18(4):452-7.
4. Hamik A, Setiadi H, Bu G, McEver RP, Morrissey JH. Down-regulation of monocyte tissue factor mediated by tissue factor pathway inhibitor and the low density lipoprotein receptor-related protein. Journal of Biological Chemistry. 1999;274(8):4962-9.
5. Oelschlager C, Romisch J, Staubitz A, Stauss H, Leithauser B, Tillmanns H, et al. Antithrombin III inhibits nuclear factor kappaB activation in human monocytes and vascular endothelial cells. Blood. 2002;99(11):4015-20.
6. Schonberg DL, Goldstein EZ, Sahinkaya FR, Wei P, Popovich PG, McTigue DM. Ferritin stimulates oligodendrocyte genesis in the adult spinal cord and can be transferred from macrophages to NG2 cells in vivo. The Journal of neuroscience : the official journal of the Society for Neuroscience. 2012;32(16):5374-84.
7. Wei SD, Zhou HC, Lin YM. Antioxidant activities of fractions of polymeric procyanidins from stem bark of Acacia confusa. International journal of molecular sciences. 2011;12(2):1146-60.
8. Smith GM, Hale JH. Macrophage/microglia regulation of astrocytic tenascin: synergistic action of transforming growth factor-β and basic fibroblast growth factor. The Journal of neuroscience. 1997;17(24):9624-33.
9. Pello OM, De Pizzol M, Mirolo M, Soucek L, Zammataro L, Amabile A, et al. Role of c-MYC in

alternative activation of human macrophages and tumor-associated macrophage biology. Blood. 2012;119(2):411-21.

10. Bruck W, Friede RL. The role of complement in myelin phagocytosis during PNS wallerian degeneration. Journal of the neurological sciences. 1991;103(2):182-7.
11. Francis K, Van Beek J, Canova C, Neal JW, Gasque P. Innate immunity and brain inflammation: the key role of complement. Expert reviews in molecular medicine. 2003;5(15):1-19.
12. Schraufstatter IU, Zhao M, Khaldoyanidi SK, DiScipio RG. The chemokine CCL18 causes maturation of cultured monocytes to macrophages in the M2 spectrum. Immunology. 2012;135(4):287-98.
13. Trentini A, Manfrinato MC, Castellazzi M, Tamborino C, Roversi G, Volta CA, et al. TIMP-1 resistant matrix metalloproteinase-9 is the predominant serum active isoform associated with MRI activity in patients with multiple sclerosis. Multiple Sclerosis Journal. 2015:1352458514560925.
14. Quélo I, Jurdic P. Differential regulation of the carbonic anhydrase II gene expression by hormonal nuclear receptors in monocytic cells: identification of the retinoic acid response element. Biochemical and biophysical research communications. 2000;271(2):481-91.
15. Gulcin I, Beydemir S. Phenolic Compounds as Antioxidants: Carbonic Anhydrase Isoenzymes Inhibitors. Mini Reviews in Medicinal Chemistry. 2013;13(3):408-30.
16. Badou A, Bennasser Y, Moreau M, Leclerc C, Benkirane M, Bahraoui E. Tat protein of human immunodeficiency virus type 1 induces interleukin-10 in human peripheral blood monocytes: implication of protein kinase C-dependent pathway. J Virol. 2000;74(22):10551-62.

17. Lee HH, Chang ZF. Regulation of RhoA-dependent ROCKII activation by Shp2. J Cell Biol. 2008: 181(6):999-1012.

18. Freywald A, Sharfe N, Rashotte C, Grunberger T, Roifman CM. The EphB6 receptor inhibits JNK activation in T lymphocytes and modulates T cell receptor-mediated responses. The Journal of biological chemistry. 2003;278(12):10150-6.

19. López-Victorio CJ, Velez-delValle C, Beltrán-Langarica A, Kuri-Harcuch W. EDF-1 downregulates the CaM/Cn/NFAT signaling pathway during adipogenesis. Biochemical and Biophysical Research Communications. 2013;432(1):146-51.

20. Bar-Or A, Nuttall RK, Duddy M, Alter A, Kim HJ, Ifergan I, et al. Analyses of all matrix metalloproteinase members in leukocytes emphasize monocytes as major inflammatory mediators in multiple sclerosis2003 2003-12-01 00:00:00. 2738-49 p.

21. Beyer M, Mallmann MR, Xue J, Staratschek-Jox A, Vorholt D, Krebs W, et al. High-resolution transcriptome of human macrophages. PloS one. 2012;7(9):e45466.

22. Booth D. Do pathogens contribute to multiple sclerosis aetiology? Microbiology Australia. 2013;34(3):144-6.

23. Miyazaki T, Morishige K, Aikawa E, Aster JC, Aikawa M. Notch3 Signaling Promotes M1 Macrophage Activation and Atherosclerosis: A Novel Therapeutic Target. Circulation. 2013;128(22 Supplement):A16302.

24. Marshall PA, Hernandez Z, Kaneko I, Widener T, Tabacaru C, Aguayo I, et al. Discovery of novel vitamin D receptor interacting proteins that modulate 1,25-dihydroxyvitamin D3 signaling. J Steroid Biochem Mol Biol. 2012;132(1-2):147-59.

25. Narvaez CJ, Matthews D, LaPorta E, Simmons KM, Beaudin S, Welsh J. The impact of vitamin D in breast cancer: genomics, pathways, metabolism. Front Physiol. 2014;5:213.

26. Lee ST, Li Z, Wu Z, Aau M, Guan P, Karuturi RK, et al. Context-specific regulation of NF-kappaB target gene expression by EZH2 in breast cancers. Mol Cell. 2011;43(5):798-810.
27. Tawara I, Sun Y, Lewis EC, Toubai T, Evers R, Nieves E, et al. Alpha-1-antitrypsin monotherapy reduces graft-versus-host disease after experimental allogeneic bone marrow transplantation. Proceedings of the National Academy of Sciences of the United States of America. 2012;109(2):564-9.
28. Gubin MM, Techasintana P, Magee JD, Dahm GM, Calaluce R, Martindale JL, et al. Conditional knockout of the RNA-binding protein HuR in CD4(+) T cells reveals a gene dosage effect on cytokine production. Mol Med. 2014;20:93-108.
29. Kovanen PE, Rosenwald A, Fu J, Hurt EM, Lam LT, Giltnane JM, et al. Analysis of gamma c-family cytokine target genes. Identification of dual-specificity phosphatase 5 (DUSP5) as a regulator of mitogen-activated protein kinase activity in interleukin-2 signaling. The Journal of biological chemistry. 2003;278(7):5205-13.